An International Journal of Optimization and Control: Theories & Applications
ISSN: 2146-0957 eISSN: 2146-5703
Vol.X, No.X, pp.X-X (2026)
https://doi.org/10.36922/IJOCTA026340224

RESEARCH ARTICLE

A surrogate model-based image-processing framework for intelligent classification of chili pepper (*Capsicum annuum* L.) products and seeds in smart agricultural systems

Kriengkrai Nabudda[1], Natakorn Thasnas[2], Elumalai Perumal Venkatesan[3,4], Sutham Craivanich[5], Pongthep Poungthong[1]*, and Suwilai Phumpho[6]

[1]Department of Industrial Engineering, School of Engineering, King Mongkut's Institute of Technology Ladkrabang, Bangkok, Thailand

[2]Department of Electrical and Computer Engineering, Faculty of Science and Engineering, Kasetsart University, Sakon Nakhon, Thailand

[3]Department of Mechanical Engineering, Aditya University, Surampalem, Andhra Pradesh, India

[4]Research Fellow, Shinawatra University, Pathum Thani, Thailand

[5]SRI-THAI-DERM Group Company Limited, Nonthaburi, Thailand

[6]Department of IoT and Information Engineering, School of Engineering, King Mongkut's Institute of Technology Ladkrabang, Bangkok, Thailand

kriang.36@gmail.com, natakorn.th@ku.th, elumalaimech89@gmail.com, srithaidermgroup@gmail.com, pongthep.po@kmitl.ac.th, suwilai.ph@kmitl.ac.th

ARTICLE INFO

Article history:
Received: August 23, 2026
Revised: September 29, 2026
Accepted: October 1, 2026
Published Online: October 16, 2026

Keywords:
Chili pepper classification
Image processing
Surrogate modeling
Edge computing
Smart agriculture
SDG 2: Zero Hunger

AMS Classification 2010:
68T05, 68T10, 90C29

ABSTRACT

Automated sorting of agricultural products requires image-classification methods that combine reliable predictive performance with computational efficiency for deployment on resource-constrained devices. This study develops a surrogate model-based image-processing framework to classify chili pepper (*Capsicum annuum* L.) products and seeds and evaluates its predictive accuracy, surrogate fidelity, and deployment efficiency. An initial dataset of 1,240 images representing green chili, fresh red chili, dried chili, and seeds was collected; after excluding 17 low-quality images, 1,223 images were analyzed. Image preprocessing and feature extraction generated a 14-dimensional representation incorporating color, texture, and morphological characteristics. MobileNetV3-Small served as the high-fidelity reference classifier, while Kriging, radial basis function (RBF), and polynomial response surface methodology (RSM) were evaluated as computationally efficient surrogates. The reference convolutional neural network achieved 97.1 ± 0.6% accuracy, compared with 95.8 ± 0.9%, 93.6 ± 1.0%, and 91.3 ± 1.2% for Kriging, RBF, and RSM, respectively. Kriging achieved the highest surrogate fidelity ($R^2 = 0.94$) while reducing inference latency from 46.2 to 5.4 ms/sample, an 8.6-fold improvement. Multi-objective optimization identified non-dominated accuracy–latency configurations for different computational constraints. The results demonstrate that surrogate selection depends on the required balance between predictive performance and computational resources. The proposed framework provides a practical basis for efficient, interpretable, and edge-deployable image classification in smart agricultural sorting systems.

CC BY

*Corresponding Author

1. Introduction

Digital transformation in agriculture through computer vision, the Internet of Things, and artificial intelligence has enabled increasingly automated approaches to crop monitoring, harvesting, sorting, and quality grading.[1-3] Among these applications, image-based classification of agricultural products and propagation materials is particularly suitable for automation because consistent, objective, and high-throughput assessment can reduce labor requirements and improve product uniformity.[1,4]

Product-stage classification identifies whole fruits by maturity or processing stage, whereas seed-stage assessment focuses on propagation material. Whole-fruit and isolated-seed images differ substantially in scale, acquisition method, feature distribution, and practical interpretation. A classifier combining these categories must therefore be evaluated cautiously, particularly when morphology provides stronger information for seed–fruit separation than for discrimination among fruit stages.

Chili pepper (*Capsicum annuum* L.) is an economically important horticultural crop worldwide and is widely cultivated for fresh and processed consumption as well as seed propagation.[5,6] Across the chili production chain, two related but distinct quality-assessment tasks are important: (i) product-stage classification, which identifies fruits according to maturity or processing stage, such as green, ripe/red, and dried chili; and (ii) seed-stage classification, which distinguishes viable and high-quality seeds from damaged or non-viable seeds before planting or commercial distribution. These tasks involve different imaging conditions, with whole-fruit imaging for product classification and isolated-seed imaging for seed assessment. Although related, they should be methodologically distinguished because their visual characteristics, feature distributions, and classification requirements differ.

Machine learning and deep learning techniques have been increasingly applied to agricultural image classification.[7-9] In particular, convolutional neural networks (CNNs) can automatically learn discriminative visual features and have achieved high classification accuracy for seeds, grains, fruits, and other agricultural materials. However, their relatively large parameter counts, memory requirements, and inference latency can limit deployment on low-cost embedded platforms, such as Raspberry Pi-based systems, microcontroller-class devices, and low-power field or conveyor-integrated sorting systems.[10,11] Consequently, practical smart-agriculture applications require not only high classification accuracy but also computational efficiency.

Surrogate modeling provides a potential alternative for reducing computational requirements. Techniques such as Kriging or Gaussian process regression, polynomial response surface methodology (RSM), and radial basis function (RBF) networks have been widely used in engineering design and optimization as computationally efficient approximations of expensive high-fidelity models.[12-14] A surrogate model approximates the input–output relationship of a more complex reference model while substantially reducing the computational cost of subsequent predictions. Despite their established use in engineering applications, surrogate models have received limited systematic investigation as efficient alternatives to deep learning models for agricultural image classification.

Three gaps motivate this study. First, Kriging, RBF, and RSM have rarely been compared with a common CNN teacher for chili classification. Second, accuracy is often reported without latency, throughput, memory, or robustness. Third, model-level timing is sometimes interpreted as system-level throughput even though acquisition, segmentation, feature extraction, communication, and actuation contribute to operational delay. Recent work on online evolutive learning similarly emphasizes the tension between adaptation and bounded real-time latency,[15] while ensemble feature aggregation illustrates the performance benefits and computational costs of combining multiple CNN representations.[16]

Accordingly, this study evaluates direct classification and knowledge-distillation modes for three surrogate families against MobileNetV3-Small. Classification performance, probability-level fidelity, interpretability, Raspberry Pi inference cost, and Pareto trade-offs are assessed within one experimental framework. The study is positioned as a controlled proof of concept. It does not claim cultivar-independent generalization, superiority over pruning or quantization, or validated end-to-end conveyor operation.

Three important research gaps therefore remain. First, surrogate modeling approaches have rarely been systematically benchmarked against a deep learning reference model for chili product and seed classification within the same data and validation protocol. Second, existing agricultural

image-classification studies commonly emphasize classification accuracy, while deployment-critical quantities such as inference latency, throughput, memory footprint, and robustness are reported less consistently. Third, conventional machine learning, deep learning, hyperspectral, and surrogate approaches are usually evaluated in separate studies, making it difficult to determine whether a modest loss in accuracy is justified by a substantial reduction in computational cost. These gaps motivate a deployment-oriented comparison in which predictive performance, fidelity to a high-capacity reference model, interpretability, and edge-computing cost are assessed together.

Accordingly, this study develops a unified framework for chili product and seed image classification that integrates image acquisition, compact color–texture–morphology feature extraction, surrogate modeling, knowledge distillation, multi-objective optimization, and graphical user interface (GUI) visualization. The specific contributions are: (i) a common benchmark of Kriging, polynomial RSM, and RBF surrogates against MobileNetV3-Small; (ii) evaluation of both direct classification and teacher-student surrogate fidelity; (iii) hardware-based measurement of accuracy–latency–memory trade-offs on a Raspberry Pi 4; (iv) Pareto-based model selection under an explicit memory constraint; and (v) robustness and GUI demonstrations that connect model benchmarking to practical smart-agriculture deployment. The objective is therefore not to claim that surrogate models universally outperform deep learning, but to establish when a compact surrogate can retain useful predictive performance while materially reducing edge-computing requirements.

2. Related work

Image-based classification has become an important component of intelligent agricultural systems because it enables rapid, non-destructive, and objective assessment of seeds and agricultural products. Previous studies have investigated a wide range of crops and materials using conventional machine learning algorithms, deep neural networks, and advanced imaging techniques. Representative studies are summarized in **Table 1**. However, these approaches differ substantially in feature representation, model complexity, computational requirements, and suitability for deployment on resource-constrained hardware. Consequently, comparing only classification accuracy provides an incomplete assessment of their practical applicability.

Deep learning approaches have demonstrated strong classification capability in agricultural applications. Researchers have applied hierarchical CNN architectures to weed-seed identification, while continual-learning CNNs have been investigated for classifying multiple crop-seed types.[7,8] These approaches benefit from automated feature learning and can accommodate complex visual variation. However, their practical deployment can require comparatively powerful computational hardware. Furthermore, although classification accuracy is commonly reported, inference latency and memory requirements are less frequently evaluated. This limitation becomes particularly important for real-time sorting systems, in which prediction speed, available memory, and processing throughput can directly determine whether a classification model can be implemented on embedded hardware.

Conventional machine learning approaches provide an alternative with lower computational complexity. Random forest and support vector machine (SVM) models have been applied to grain and fruit classification using manually or computationally extracted color, shape, and texture features.[9,17] Hyperspectral imaging combined with partial least-squares discriminant analysis has also been investigated for seed-quality assessment.[18] These studies demonstrate that informative image-derived features can provide effective classification without necessarily requiring deep neural networks. Nevertheless, the relationship between feature representation, model complexity, predictive accuracy, and deployment cost remains insufficiently characterized for chili product and seed classification. Moreover, differences in datasets, imaging conditions, validation procedures, and computing platforms make direct comparison among reported accuracies difficult.

Surrogate modeling offers another potentially useful strategy. Unlike conventional classifiers that are trained directly for classification, surrogate models can approximate the response of a high-fidelity reference model using a reduced computational representation. Kriging or Gaussian process regression, polynomial RSM, and RBF models are widely used as computationally efficient approximations of expensive high-fidelity models.[12-14] However, their application to agricultural image classification remains limited, and direct comparisons with high-fidelity reference models are scarce. The three

surrogate families also provide different modeling characteristics. Kriging offers flexible nonlinear approximation and probabilistic prediction, RBF models capture nonlinear relationships through localized basis functions, whereas polynomial RSM provides a simpler analytical representation with very low computational requirements. These differences make a common comparison particularly relevant when both predictive performance and computational efficiency are considered.

From an engineering–model–reduction perspective, the same surrogate philosophy is used when a computationally expensive reference model is replaced by a lower-cost approximation for repeated prediction and optimization. This study transfers that design logic to agricultural image classification: MobileNetV3-Small supplies the high-fidelity probability response, while Kriging, RBF, and polynomial RSM approximate the descriptor-to-response relationship. The purpose is therefore not to claim physics-informed image classification, but to evaluate whether established surrogate-model selection concepts can support accuracy–latency–memory trade-offs on resource-constrained hardware.

A further distinction concerns the relationship between classification accuracy and surrogate fidelity. A reduced model may correctly predict the final class while not reproducing the response behavior of the underlying high-fidelity model. Conversely, a surrogate that closely reproduces the reference-model output may provide useful information for model compression and knowledge transfer. Therefore, evaluating surrogate models against both ground-truth class labels and reference-model predictions provides a more complete assessment than classification accuracy alone. In this study, this distinction is quantified through conventional classification metrics together with root mean squared error (RMSE), mean absolute error (MAE), and R^2 measures of surrogate fidelity.

A further limitation of previous studies is the lack of integrated evaluation of accuracy and computational efficiency. For practical deployment in smart sorting and agricultural monitoring systems, a model with slightly lower accuracy may be preferable if it provides substantially lower inference latency and memory requirements. Conversely, a highly accurate model may be unsuitable for resource-constrained edge hardware if its computational demand is excessive. Therefore, model selection should consider multiple performance dimensions rather than classification accuracy alone. In addition to accuracy, latency, and memory, model interpretability and robustness to changes in image-acquisition conditions are important because agricultural products exhibit biological variability and practical imaging environments cannot always reproduce laboratory conditions.

Table 1 provides a direct comparison with representative approaches in the literature. Deep learning studies[7,8] reported accuracies of 93.2% and 91.8%, respectively, whereas conventional feature-based approaches using random forest, SVM, and partial least-squares discriminant analysis reported accuracies ranging from 88.1% to 92.5%.[9,17,18] However, inference latency was not reported for these representative studies. In contrast, the present framework evaluates multiple surrogate architectures against a high-fidelity reference while explicitly considering classification performance, surrogate fidelity, and computational cost. This comparison is not intended to claim superiority based solely on numerical accuracy because the studies use different datasets and experimental conditions. Rather, it identifies the methodological distinction of the present work: predictive and computational characteristics are evaluated simultaneously within the same dataset, validation procedure, and hardware environment.

Recent studies support multi-objective optimization and feature-importance analysis to balance engineering objectives and improve model interpretability.[19,20] Surrogate-assisted computational fluid dynamics studies in wire coating and refrigerated transport further demonstrate the value of reference-model/ surrogate frameworks for reducing computational cost and supporting performance–resource optimization.[21,22]

Deployment-oriented agricultural vision studies emphasize evaluating accuracy together with embedded processing and operational requirements.[23,24] Surrogate-assisted optimization can reduce computational cost in engineering applications,[25-27] while Edge artificial intelligence performance depends on model architecture, hardware, and the complete processing pipeline.[28] Multi-objective approaches further support explicit accuracy–latency–resource trade-offs[29,30], including resource-aware agricultural applications.[31,32] Recent seed-classification studies demonstrate efficient deep learning and machine vision approaches,[33,34] whereas knowledge distillation can reduce edge-computing demand but requires comparison with alternative

compression methods.[35] Federated learning may additionally support future multi-site agricultural deployment, although communication and hardware heterogeneity remain important considerations.[36]

The contribution of the present study therefore does not arise from introducing Kriging, RSM, RBF, or image classification as individual techniques. Instead, it lies in establishing a unified surrogate-based framework in which these models are evaluated under identical experimental conditions against a common high-fidelity reference. The framework combines classification accuracy, surrogate fidelity, feature-level interpretability, experimentally measured inference latency and memory requirements, robustness assessment, and multi-objective optimization. This enables the model-selection problem to be formulated as an accuracy–latency–memory trade-off rather than an accuracy-only comparison.

Accordingly, the present study addresses the identified gaps by establishing a common experimental framework in which Kriging, polynomial RSM, and RBF surrogate models are evaluated against a high-fidelity reference model for chili product and seed classification. Beyond classification accuracy, the framework evaluates surrogate fidelity and experimentally measured computational cost, including inference latency and memory requirements. This enables the identification of accuracy–efficiency trade-offs and provides a practical basis for selecting classification architectures according to available hardware resources. By integrating surrogate benchmarking, interpretability, robustness evaluation, edge-hardware measurements, and Pareto-based model selection, the proposed framework extends previous agricultural image-classification research from accuracy-oriented benchmarking toward deployment-oriented model selection for resource-constrained smart-agriculture systems.

Broader reviews of machine learning and deep learning in smart connected systems show that accuracy often takes priority over scalability, resource demand, and operational constraints.[21] Reviews of pattern recognition in cyber–physical–social systems similarly identify adaptability, flexibility, fault tolerance, and scalability

Table 1. Comparison with representative state-of-the-art agricultural image-classification studies

Study	Crop/ material	Feature type	Model	Dataset size	Reported accuracy	Latency reported	Principal focus
7	Weed seeds	Deep features	Hierarchical bilinear convolutional neural network	5,000+	93.2%	No	Deep-learning classification
8	Multiple crop seeds	Pixel-level	Continual-learning convolutional neural network	3,200	91.8%	No	Continual classification
9	Grain kernels	Color + shape	Random forest	1,800	89.4%	No	Feature-based machine learning
15	Fruit ripeness	Color histograms	Support vector machine	900	88.1%	No	Ripeness classification
16	Rice seed vigor	Hyperspectral	Partial least-squares discriminant analysis	600	92.5%	No	Spectral seed assessment
This study	Chili product + seed	Color + texture + morphology	Kriging/ response surface methodology/ radial basis function vs. convolutional neural network	1,240	95.8% (best surrogate)	Yes	Accuracy–fidelity–computational-efficiency trade-off and edge deployment

as relevant evaluation dimensions.[22] These observations support a multi-criteria evaluation, but they do not remove the need for direct baselines using identical data and hardware.

Recent studies emphasize evaluating agricultural vision beyond accuracy by considering embedded processing and operational requirements.[25,26] Surrogate optimization supports efficient multi-objective decision-making,[27-29,31,32,34] while Edge artificial intelligence highlights architecture-, hardware-, and pipeline-dependent performance.[30,33] Recent work also advances seed classification,[35,36] knowledge distillation, and federated learning for compact and distributed edge intelligence.[37,38]

3. Materials and methods

3.1. Plant material and image acquisition

Chili fruits and seeds (*Capsicum annuum* L., cv. "Cakra Hijau") were obtained from one commercial farm in Thailand in three batches over two months. Four classes were defined: green chili, fresh red chili, dried chili, and isolated seeds. The initial dataset contained 310 images per class (1,240 images). Whole-fruit images were acquired with a fixed-mount 12-MP RGB camera at 4,000 × 3,000 pixels, positioned 25 cm above a matte-black background and illuminated by a diffuse 5,500 K light-emitting diode ring light. Seed images were obtained with a 600-dpi flatbed scanner; seeds were separated before Otsu thresholding and watershed processing.

Seventeen images were excluded because of severe motion blur, incomplete foreground segmentation, excessive reflection or shadow, or target truncation. The retained dataset comprised 305 green chili, 308 fresh red chili, 302 dried chili, and 308 isolated-seed images. The available records did not permit a verified count of distinct biological specimens or confirm whether repeated views of the same specimen crossed data partitions. Consequently, the reported validation is image-level and may be optimistic if correlated views were present. Future datasets should assign persistent specimen identifiers and use specimen-grouped partitioning.

3.2. Image preprocessing

All images underwent four preprocessing steps: (i) background segmentation using Otsu thresholding on the grayscale channel; (ii) noise suppression using a 3 × 3 Gaussian filter; (iii) conversion from RGB to HSV and CIE Lab color spaces for illumination-robust feature computation; and (iv) size normalization. Images were resized to 224 × 224 pixels for CNN input, whereas morphological measurements were retained at native resolution using a pixel-to-millimeter calibration factor obtained from a reference scale bar included during each acquisition session.[39,40]

The descriptor vector contained 17 variables: the mean and standard deviation of the R, G, and B channels (six); mean hue, saturation, and value (three); gray-level co-occurrence matrix (GLCM) contrast, homogeneity, energy, and correlation plus local binary pattern uniformity (five); and foreground area, eccentricity, and solidity (three). Morphological descriptors were calculated from the segmented foreground mask for every image, not only after class assignment. They are expected to contribute more strongly to seed–fruit separation than to discrimination among the three fruit classes. All variables were standardized using parameters estimated from training data.

3.3. High-fidelity reference model

MobileNetV3-Small, pretrained on ImageNet, was fine-tuned on raw RGB images using Adam (learning rate 1×10^{-4}, batch size 32, maximum 50 epochs, and early-stopping patience of eight epochs). The CNN generated a four-component softmax vector for each image.

The surrogate models received the 17-dimensional handcrafted vector rather than CNN intermediate features. In direct mode, each surrogate learned the mapping from descriptors to ground-truth class labels. In distillation mode, it learned the mapping from the descriptor vector to the four CNN softmax probabilities. Thus, the CNN served as a probability-generating teacher. Logits and hidden CNN representations were not supplied to the surrogates.

3.4. Surrogate model formulations

For a high-fidelity system output expressed as $y = f(\mathrm{X}) + \varepsilon$, the surrogate output was defined as $\hat{y} = \hat{f}(\mathrm{X})$, where $\hat{f}$ approximates the reference function at reduced computational cost. Three surrogate approaches were implemented.

(i) Kriging (Gaussian process regression): Kriging was formulated as a Gaussian process with mean function $\mu(\mathrm{X})$ and covariance kernel $k(\mathrm{X}_i, \mathrm{X}_j)$. A Matérn kernel with $\nu = 2.5$ was selected to provide a balance between smoothness and flexibility. Kernel length scale, signal variance, and noise variance were

optimized by maximum marginal likelihood (**Equation 1**):

$$k\left(X_i, X_j\right) = \sigma^2\left(1+\frac{\sqrt{5}d}{\ell}+\frac{5d^2}{3\ell^2}\right)\exp\left(-\frac{\sqrt{5}d}{\ell}\right),$$

$$d = \| X_i - X_j \tag{1}$$

Kernel hyperparameters (length scale ℓ, signal variance σ^2, noise variance) were optimized via maximum marginal likelihood.

(ii) Polynomial RSM: A second-order polynomial response surface was fitted to the extracted features (**Equation 2**):

$$\hat{y} = \beta_0 + \sum_{i=1}^{14}\beta_i x_i + \sum_{i=1}^{14}\beta_{ii}x_i^2 + \sum_{i<j}\beta_{ij}x_i x_j + \varepsilon \tag{2}$$

Model coefficients were estimated using ordinary least squares, with a multinomial logistic link for the classification setting. Statistical significance was assessed using analysis of variance at $\alpha = 0.05$.

(iii) RBF network: The RBF surrogate was represented as a weighted sum of Gaussian basis functions centered at M representative points c_m. The centers were selected by k-means clustering, with $M = 40$ determined by cross-validation (**Equation 3**):

$$\hat{y} = \sum_{m=1}^{M} w_m \exp\left(-\gamma \left\| X - c_m \right\|^2\right) \tag{3}$$

The weights were estimated using regularized least squares, and the kernel width γ was optimized using a grid search with five-fold inner cross-validation.

Each surrogate was trained in two modes: (i) direct mode, in which the model was fitted to ground-truth class labels; and (ii) distillation mode, in which the model was fitted to the CNN softmax output distribution. The latter enabled explicit evaluation of surrogate fidelity to the high-fidelity reference model.

3.5. Multi-objective optimization

A bi-objective optimization problem was formulated to maximize classification accuracy, $A(\vartheta)$, while minimizing inference latency, $T(\vartheta)$, as functions of surrogate hyperparameters ϑ. The optimization was subject to a peak memory-footprint constraint of ≤50 MB, representing a practical resource limit for embedded deployment. Non-dominated sorting genetic algorithm II (NSGA-II) was used with a population size of 60, 100 generations, crossover probability of 0.9, and mutation probability of 0.1. The resulting Pareto fronts identified non-dominated hyperparameter configurations for each surrogate family.

MobileNetV3-Small received the resized RGB image and generated a four-element softmax probability vector, p_i^{CNN}. In distillation mode, each surrogate received the corresponding standardized handcrafted vector, $x_i \in R^{14}$, and learned the mapping $\hat{f}: x_i \rightarrow p^{CNN}$. The surrogate output was normalized to obtain a valid class-probability distribution, and its predicted class was determined by the maximum-probability component. No CNN logits or intermediate feature representations were supplied to the surrogate. In direct mode, the same handcrafted input vector was mapped to the one-hot ground-truth label instead of the teacher probability distribution.

3.6. Experimental design and evaluation metrics

The retained images were partitioned using stratification into 90% development and 10% held-out test subsets. Ten-fold cross-validation was repeated over five random seeds, producing 50 image-level partitions. Accuracy, macro-precision, macro-recall, macro-F1, and Cohen's $\varkappa$ were calculated. The nearly balanced class counts reduce, but do not eliminate, the need for per-class evaluation. The absence of specimen identifiers prevented specimen-grouped cross-validation and was treated as a limitation rather than concealed as specimen-independent validation.

Probability-level teacher fidelity was assessed with RMSE, MAE, and R^2 between CNN and surrogate probability outputs. R^2 describes reproduction of continuous probability variance; it is not itself a multiclass performance measure. Decision-level agreement and confusion matrices were therefore examined separately. Future reporting should add Jensen–Shannon divergence, teacher–surrogate Cohen's $\varkappa$, and class-wise agreement.

Pairwise differences across matched partitions were assessed with Wilcoxon signed-rank tests at $\alpha = 0.05$ with Holm–Bonferroni correction. Permutation importance was estimated across cross-validation partitions. Conventional classifiers trained on the same descriptors and compressed CNN variants were not included; accordingly, the study does not establish a unique advantage over logistic regression, SVM, random forest, gradient boosting, k-nearest neighbors, compact multilayer perceptron, pruning, or quantization.

3.7. Edge benchmarking and multi-objective optimization

Computational measurements were obtained on a Raspberry Pi 4 Model B with 4 GB RAM and a Broadcom BCM2711 quad-core Cortex-A72 processor at 1.5 GHz. The implementation used Python 3.11, OpenCV 4.9, scikit-learn 1.4, scikit-optimize, PyTorch 2.2, and pymoo 0.6. Reported latency covers model inference for one prepared sample and excludes image exposure, transfer, segmentation, handcrafted-feature calculation, model loading, GUI rendering, network communication, conveyor tracking, and actuator response. The reported throughput is therefore model-level inference throughput, not sorting-line throughput.

Non-dominated sorting genetic algorithm II maximized cross-validated accuracy and minimized inference latency subject to peak memory ≤50 MB. It used a population of 60, 100 generations, a crossover probability of 0.9, and a mutation probability of 0.1. Decision variables were model family and family-specific hyperparameters, including Kriging kernel parameters, RBF center count and width, and polynomial configuration. The generated Pareto front supports constraint-dependent selection; because the original experiment did not define a formal knee-point or utility rule, no single universal operating point is claimed.

4. Results

4.1. Dataset composition

Table 2 summarizes the retained image-level dataset and the development and held-out partitions used in the reported evaluation.

The reference model correctly classified all 122 images in this held-out split. This 100% result is reported only as a split-specific observation and should not be interpreted independently of repeated cross-validation or as evidence of external generalization.

4.2. Model interpretability and feature importance

Figure 1 presents a global interpretability analysis using an approximating surrogate decision tree. The resulting tree revealed a clear hierarchical classification structure in which seed density was the dominant first-level discriminator, followed by texture and color characteristics. Samples with seed density greater than 0.495 were classified as isolated seeds, producing a pure terminal node containing 277 samples (Gini = 0.0). Among samples with seed density ≤0.495, texture score provided the next major separation. Lower texture values were primarily associated with fresh chili classes, whereas higher texture values were associated with dried chili. Hue and saturation subsequently distinguished fresh red chili from green chili, while brightness further refined the classification of dried samples.

Figure 2 shows the confusion matrix obtained from the held-out test set of 122 samples. All 30 green chili, 31 fresh red chili, 30 dried chili, and 31 isolated seed samples were correctly classified, resulting in an overall accuracy of 100% on this particular test set. Precision, recall, and F1-score were consequently 1.00 for all four classes.

Figure 3 evaluates surrogate fidelity by comparing surrogate predictions with the predictions of the underlying black-box classifier. The surrogate reproduced 120 of 122 black-box predictions, corresponding to a global fidelity of 98.36%. Complete agreement was obtained for green chili (30/30), fresh red chili (31/31), and isolated seeds (31/31). For dried chili, 28 of 30 predictions were reproduced, with two disagreements involving green chili and fresh red

Table 2. Final image-level dataset composition

Class	Retained	Development (90%)	Held-out (10%)
Green chili	305	275	30
Fresh red chili	308	277	31
Dried chili	302	272	30
Isolated seeds	308	277	31
Total	1,223	1,101	122

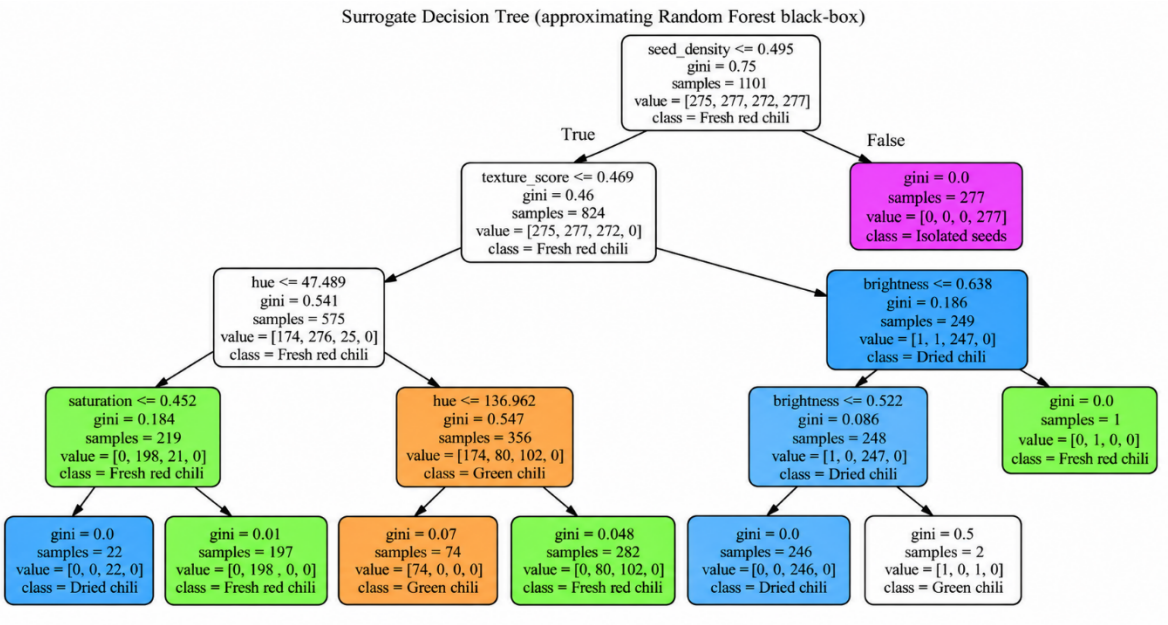


Figure 1. Global interpretability visualization of the classifier using an approximating surrogate decision tree

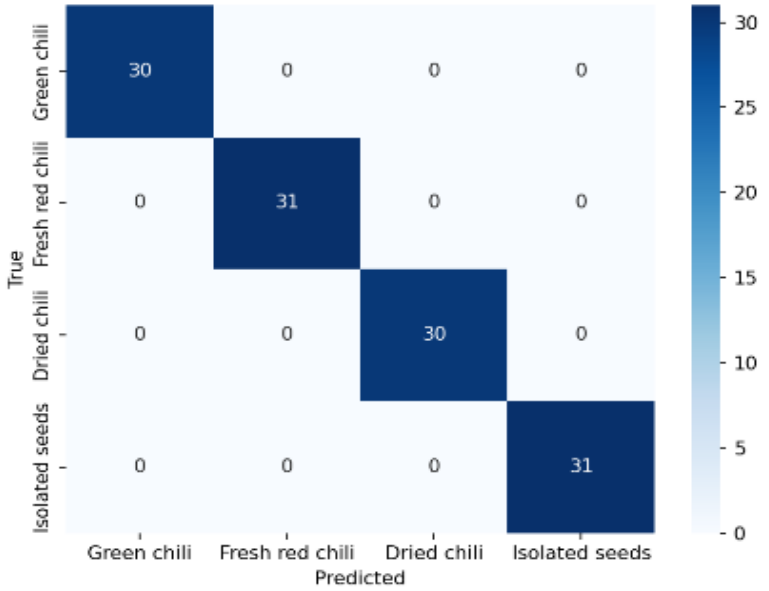


Figure 2. Confusion matrix evaluating classification performance on the held-out test dataset

chili predictions.

Figure 4 shows that the surrogate reproduced 120 of 122 teacher decisions (98.36% agreement). Against ground truth, it correctly classified all green, fresh red, and seed images in this split and 28 of 30 dried chili images. These confusion matrices supplement, but do not replace, repeated cross-validation.

Figure 5 presents the Gini-based feature-importance ranking derived from the surrogate decision tree. Seed density was the most influential feature (0.338), followed by hue (0.325) and texture score (0.287). Saturation contributed 0.048, whereas brightness contributed 0.004. Thus, seed density, hue, and texture score together accounted for more than 95% of the total feature importance.

Table 3 provides the cross-validated permutation importance of the seven most influential features. Grayscale standard deviation

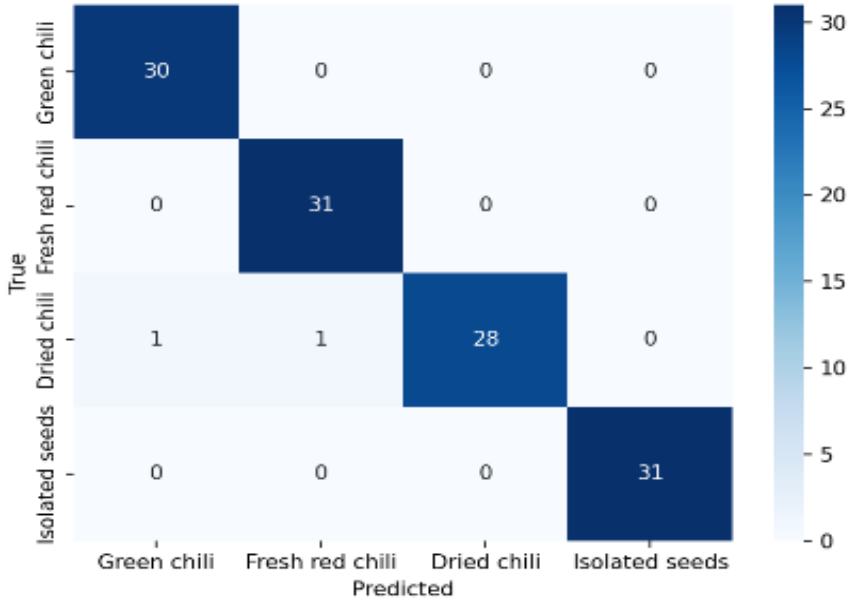


Figure 3. Surrogate fidelity confusion matrix comparing surrogate predictions with black-box model predictions

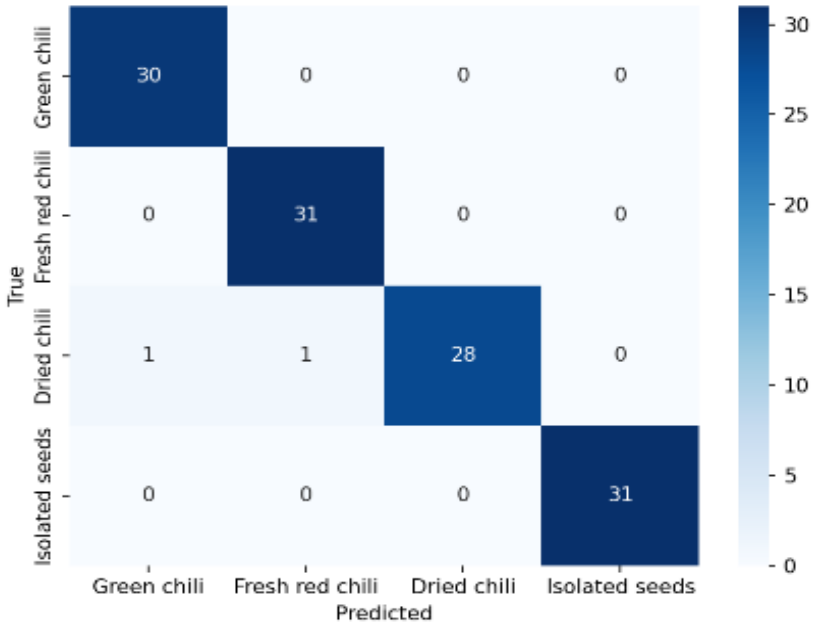


Figure 4. Confusion matrix of the surrogate decision tree against ground-truth class labels

exhibited the highest mean importance (0.194 ± 0.021), followed by mean HSV saturation (0.161 ± 0.018), GLCM contrast (0.133 ± 0.015), mean HSV value (0.109 ± 0.014), mean R-channel intensity (0.087 ± 0.012), GLCM homogeneity (0.071 ± 0.010), and local binary pattern uniformity (0.058 ± 0.009). The results indicate that grayscale variability, color saturation, and surface-texture descriptors were particularly informative for distinguishing the four chili categories.

4.3. Classification performance

Table 4 summarizes the classification performance of MobileNetV3-Small and the three surrogate models across the 50 image-level cross-validation partitions. The cross-validated results in **Table 4** complement the performance presented in **Figure 2**, providing a more comprehensive assessment of model robustness

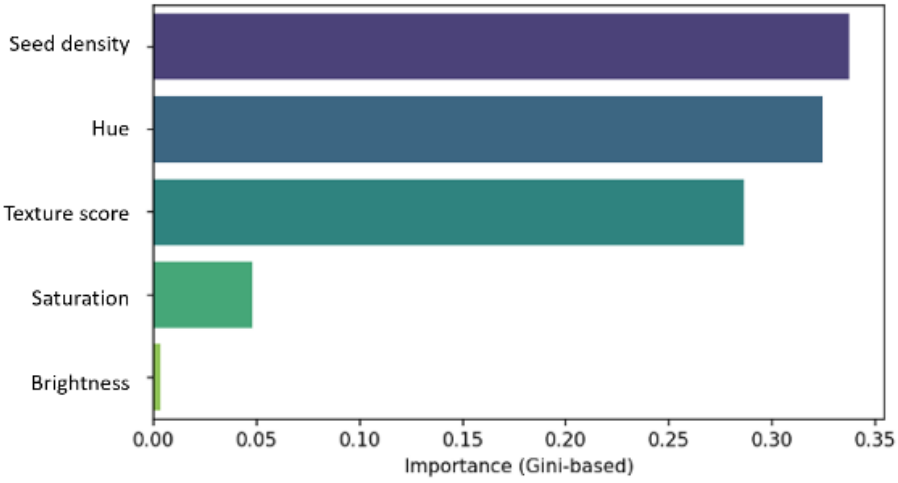


Figure 5. Feature-importance ranking derived from the surrogate decision tree

Table 3. Cross-validated permutation importance (mean ± standard deviation, $n = 50$ cross-validated partitions)

Rank	Feature	Importance
1	Grayscale standard deviation	0.194 ± 0.021
2	HSV saturation (mean)	0.161 ± 0.018
3	Gray-level co-occurrence matrix contrast	0.133 ± 0.015
4	HSV value (mean)	0.109 ± 0.014
5	Mean R channel	0.087 ± 0.012
6	Gray-level co-occurrence matrix homogeneity	0.071 ± 0.010
7	Local binary pattern uniformity	0.058 ± 0.009

Table 4. Classification performance across 50 image-level cross-validation partitions (mean ± standard deviation)

Model	Accuracy	Precision	Recall	F1	ϰ
MobileNetV3-Small	0.971 ± 0.006	0.969 ± 0.007	0.970 ± 0.006	0.969 ± 0.007	0.961 ± 0.008
Kriging	0.958 ± 0.009	0.955 ± 0.010	0.957 ± 0.009	0.956 ± 0.010	0.944 ± 0.012
Radial basis function	0.936 ± 0.010	0.932 ± 0.011	0.934 ± 0.011	0.933 ± 0.011	0.915 ± 0.014
Polynomial response surface methodology	0.913 ± 0.012	0.908 ± 0.013	0.910 ± 0.012	0.909 ± 0.013	0.884 ± 0.016

and generalization beyond the held-out test partition.

The CNN achieved the highest mean accuracy, followed by Kriging, RBF, and RSM. The CNN–Kriging difference was not statistically significant under the reported Wilcoxon procedure (adjusted $p = 0.087$), whereas RBF and RSM differed from the CNN (adjusted $p < 0.001$). These tests apply to matched image-level partitions and do not correct for possible specimen correlation.

Table 5 reports the probability-level fidelity of each surrogate relative to MobileNetV3-Small using RMSE, MAE, and R^2.

Kriging most closely reproduced the CNN probability outputs. These values should not be interpreted as substitutes for classification agreement, calibration, or divergence measures.

4.4. Computational performance and Pareto analysis

Table 6 summarizes model-level training time, inference latency, throughput, and peak memory measured on the Raspberry Pi 4.

Relative to the CNN, Kriging reduced model-inference latency by approximately 8.6-fold. This comparison excludes preprocessing and actuation. Model-file size, energy per inference, numerical precision, warm-up count, and percentile latency were not available in the source records and should be included in a future reproducible benchmark.

4.5. Model interpretability and feature importance

The NSGA-II optimization produced a Pareto front spanning the accuracy–latency trade-off shown in **Figure 6**. Kriging configurations occupied the high-accuracy region, achieving approximately 95% or higher accuracy at latencies of approximately 4 ms or above. RBF configurations occupied the intermediate region, with approximately 92%–94% accuracy at 2–3 ms latency. Polynomial RSM configurations occupied the ultra-low-latency region, with latencies below 2 ms and accuracy of approximately 88%–91%. These results demonstrate that model selection depends on the required balance between predictive accuracy and computational resources.

4.6. Robustness and interface demonstration

An independent robustness set of 180 images was acquired under ±30% illumination variation and two alternative backgrounds. Accuracy decreased by 3.2 percentage points for the CNN, 4.7 for Kriging, 6.1 for RBF, and 7.8 for RSM. The set did not systematically examine motion blur, partial occlusion, overlapping products, surface contamination, camera or conveyor vibration, fruit orientation, or belt speed.

Table 5. Probability-level surrogate fidelity relative to MobileNetV3-Small

Surrogate	Root mean squared error	Mean absolute error	R^2
Kriging	0.081	0.062	0.94
Radial basis function	0.114	0.089	0.88
Response surface methodology	0.147	0.121	0.79

Table 6. Model-level computational performance on Raspberry Pi 4

Model	Training time	Latency (ms/ sample)	Throughput (samples/s)	Peak memory
MobileNetV3-Small	42 min	46.2 ± 2.1	21.6	9.8 MB
Kriging	3.1 min	5.4 ± 0.4	185.2	4.1 MB
Radial basis function	1.4 min	2.8 ± 0.3	357.1	1.6 MB
Response surface methodology	0.4 min	1.1 ± 0.1	909.1	0.3 MB

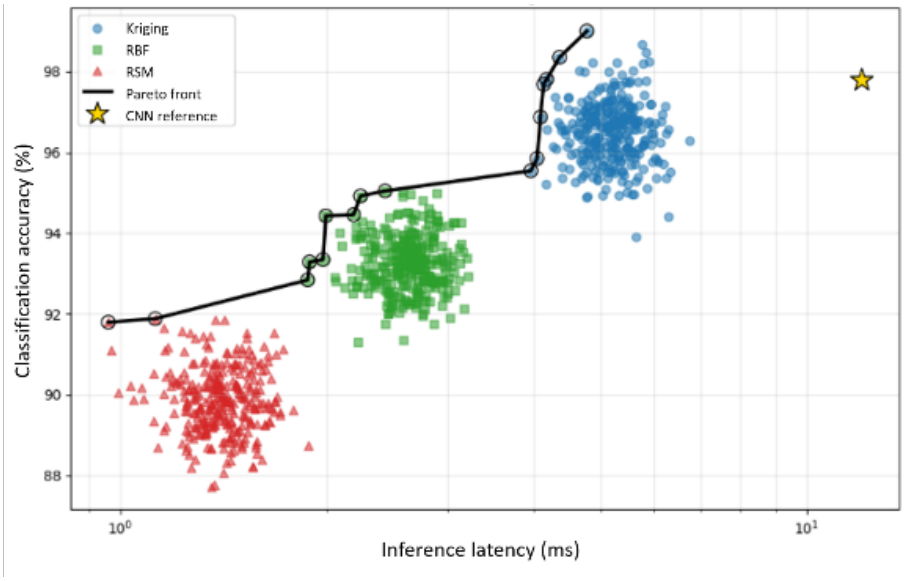


Figure 6. Pareto front plot, accuracy (y-axis) vs. inference latency (x-axis, log scale), with distinct markers for Kriging, radial basis function (RBF), and response surface methodology (RSM) configurations; convolutional neural network (CNN) reference plotted as a fixed reference point

4.7. Dashboard demonstration

Figure 7 illustrates the developed GUI for practical deployment of the surrogate model-based image-processing framework. The interface integrates image acquisition, automated feature extraction, surrogate-model inference, and visualization of classification results. Users can upload four images and specify the expected target categories before initiating analysis. The processed images are displayed in a four-panel preview, while the computer-vision pipeline extracts quantitative descriptors including mean grayscale intensity, grayscale standard deviation, mean hue, mean saturation, mean HSV value, and edge density. The resulting feature vectors are supplied to the surrogate model to generate real-time classifications and associated feature information.

In the demonstrated examples, the system identified green chili, fresh red chili, dried chili, and chili seeds using the extracted image features. The GUI demonstrates software integration and operator-facing visualization. It is not evidence of real conveyor throughput because tracking, controller communication, and mechanical actuation were not included.

5. Discussion

5.1. Principal findings and interpretation

The results show that compact surrogates can approximate a MobileNetV3-Small teacher while reducing model-level inference cost on Raspberry Pi 4. Kriging retained the highest accuracy and fidelity, RBF offered an intermediate trade-off, and RSM minimized latency and memory. The contribution is therefore a common accuracy–fidelity–resource evaluation, not proof that surrogates universally outperform deep learning or conventional feature-based classifiers.

Color and texture distinguish maturity and drying states, whereas morphology contributes principally to seed–fruit separation. Computing morphology on every foreground mask avoids class-conditional feature availability, but unequal feature utility remains. A fruit-only ablation and a feature-family ablation are needed to quantify incremental value without allowing the easily separated seed class to dominate aggregate importance.

5.2. Direct learning, distillation, and missing baselines

Distillation transfers continuous teacher probabilities, which contain information about relative class similarity that one-hot labels omit. Nevertheless, the present comparison cannot isolate a unique distillation advantage because logistic regression, SVM, random forest, XGBoost, k-nearest neighbors, and a compact multilayer perceptron were not trained on the same descriptor vector. A rigorous extension should compare these baselines using identical

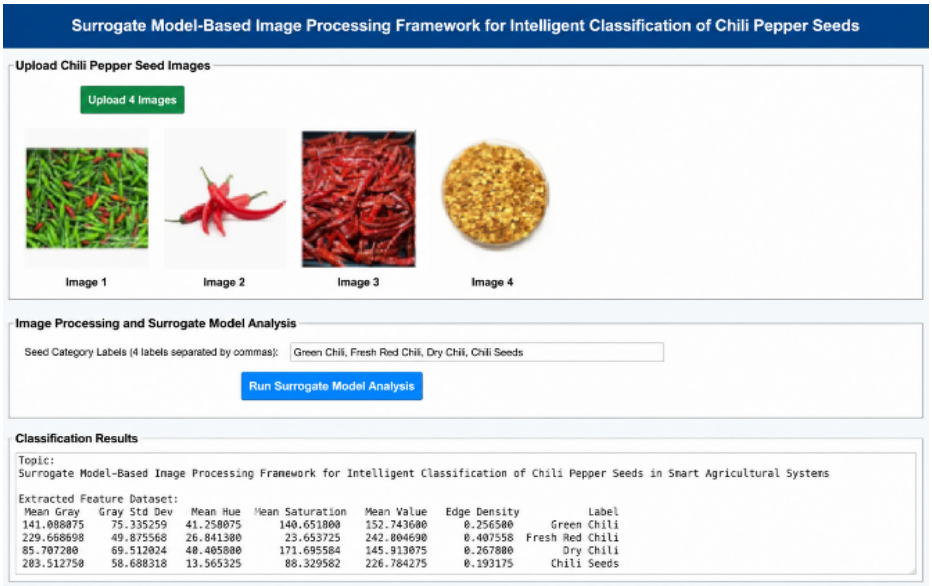


Figure 7. Screenshots of the graphical user interface dashboard showing the classification output with predicted class, confidence score, and feature-importance visualization

specimen-grouped partitions and report ground-truth performance, teacher agreement, memory, latency, and calibration.

The study also lacks pruning and quantization baselines. Compressed CNNs retain learned image representations and may avoid dependence on handcrafted segmentation, whereas surrogates reduce inference cost after a separate feature pipeline. Only end-to-end timing and energy measurements can establish which pathway is preferable.

5.3. Scalability and deployment boundaries

Exact Kriging commonly requires $O(n^3)$ training time and $O(n^2)$ storage for covariance factorization, with prediction cost increasing with the number of retained observations. Its favorable performance at the present scale may therefore deteriorate for larger datasets. Sparse Gaussian processes, inducing-point methods, local experts, or representative-subset selection should be considered. RBF cost depends on the number of centers, whereas RSM offers low prediction cost at the expense of limited nonlinear flexibility.

The reported latency measurements apply only to model inference. Operational sorting additionally requires image acquisition, segmentation, feature extraction, tracking, communication, decision logic, actuation, and verification. Future conveyor experiments should therefore evaluate end-to-end latency, sorting accuracy, throughput, energy consumption, and performance across different belt speeds and object spacings.

From an industrial-engineering perspective, the complete sorting-cycle time can be expressed conceptually as **Equation 4**:

$$T_{\text{cycle}} = T_{\text{capture}} + T_{\text{transfer}} + T_{\text{segment}} + T_{\text{features}} + T_{\text{infer}} + T_{\text{control}} + T_{\text{actuate}} \quad (4)$$

The present benchmark quantifies only T_{infer}. Therefore, the observed surrogate speed-up represents model-level computational acceleration and should not be interpreted directly as an increase in conveyor throughput until the remaining system-level components are measured.

5.4. Limitations and future work

The dataset represents one cultivar from one farm and a narrow collection interval. Three batches capture limited within-domain variation but do not represent genetic, geographical, seasonal, or production-system diversity. The image-level validation may be optimistic if repeated views of a specimen cross folds. The robustness set covered only illumination and background, and the GUI is not a physical sorting system.

Future work should establish specimen identifiers at acquisition; use multi-cultivar, multi-farm, multi-season, and multi-camera external datasets; perform specimen-grouped nested

validation; include conventional lightweight and compressed-CNN baselines; add class-wise specificity, balanced accuracy, confidence intervals, calibration, and distribution-divergence measures; quantify energy and end-to-end latency; and validate on a conveyor with realistic blur, occlusion, contamination, vibration, speed, and actuator constraints. Online adaptation may subsequently be examined, provided that update cost and bounded latency are evaluated together.[15]

6. Conclusion

This study developed a controlled proof-of-concept framework for classifying green chili, fresh red chili, dried chili, and isolated seeds using compact surrogates benchmarked against MobileNetV3-Small. Kriging achieved the strongest surrogate performance (95.8 ± 0.9% accuracy; $R^2 = 0.94$) and reduced model-inference latency from 46.2 ± 2.1 to 5.4 ± 0.4 ms per sample on Raspberry Pi 4. RBF and RSM occupied progressively lower-latency regions with larger accuracy reductions. NSGA-II identified non-dominated configurations under a memory constraint, demonstrating that architecture selection depends on application-specific priorities rather than accuracy alone.

The findings support feasibility under the tested laboratory and moderate acquisition perturbations, but they do not demonstrate cultivar-independent generalization, specimen-independent accuracy, superiority over conventional lightweight or compressed CNN alternatives, or complete conveyor-system performance. These boundaries are central to interpretation. Multi-cultivar external validation, grouped evaluation, ablation studies, compression and lightweight-classifier benchmarks, and end-to-end conveyor testing are required before industrial adoption.

Acknowledgments

We thank SRI-THAI-DERM Co., Ltd. for its support in project implementation.

Funding

This work was funded by the Research and Innovation Acceleration Agency for Competitiveness and Area Development (RCAD), Thailand, through the Program Management Unit for Competitiveness (PMU-C), contract number C05F690074.

Conflict of interest

The authors declare that they have no conflict of interest.

Author contributions

Conceptualization: Kriengkrai Nabudda, Natakorn Thasnas, Pongthep Poungthong, Suwilai Phumpho
Data curation: Kriengkrai Nabudda, Natakorn Thasnas
Formal analysis: Kriengkrai Nabudda, Elumalai Perumal Venkatesan, Pongthep Poungthong
Investigation: Kriengkrai Nabudda, Natakorn Thasnas, Sutham Craivanich
Methodology: Kriengkrai Nabudda, Natakorn Thasnas, Pongthep Poungthong
Supervision: Elumalai Perumal Venkatesan, Suwilai Phumpho
Visualization: Natakorn Thasnas, Pongthep Poungthong, Suwilai Phumpho
Writing–original draft: Kriengkrai Nabudda, Pongthep Poungthong
Writing–review & editing: All authors

Availability of data

The data supporting the findings of this study are available from the corresponding author upon reasonable request.

AI tools statement

OpenAI ChatGPT was used solely to assist with English-language editing, clarity, consistency checking, and presentation of the revised manuscript. It was not used to generate, fabricate, or modify experimental data, statistical results, model outputs, or scientific conclusions. All AI-assisted text was critically reviewed and edited by the authors, who take full responsibility for the accuracy and integrity of the manuscript.

References

1. Cravero A, Sepúlveda S, Gutiérrez F, Muñoz L. From precision agriculture to intelligent agricultural ecosystems: a systematic review of machine learning and big data applications. *Agronomy*. 2026;16(5):516.

   https://doi.org/10.3390/agronomy16050516

2. Miller T, Mikiciuk G, Durlik I, Mikiciuk M, Łobodzińska A, Śnieg M. The IoT and AI in agriculture: the time is now—a systematic review of smart sensing technologies. *Sensors (Basel)*.

2025;25(12):3583.

https://doi.org/10.3390/s25123583

3. Olorunfemi BO, Nwulu NI, Adebo OA, Kavadias KA. Advancements in machine visions for fruit sorting and grading: a bibliometric analysis, systematic review, and future research directions. *J Agric Food Res.* 2024;16:101154.

   https://doi.org/10.1016/j.jafr.2024.101154

4. Azadpour A, Mollazade K, Ramezani M, Samimi-Akhijahani H. Automated grading of oleaster fruit using deep learning. *Sci Rep.* 2025;15(1).

   https://doi.org/10.1038/s41598-025-89358-6

5. Tai S, Tang Z, Li B, Wang S, Guo X. Intelligent recognition and automated production of chili peppers: a review addressing varietal diversity and technological requirements. *Agriculture.* 2025;15(11):1200.

   https://doi.org/10.3390/agriculture15111200

6. Peng Y, Zhou Y, Zhang L, *et al.* Seed non-destructive intelligent detection technology: a review of current status, advances, and future directions. *J Food Compos Anal.* 2026;156:109300.

   https://doi.org/10.1016/j.jfca.2026.109300

7. Yang L, Yan J, Cao X, *et al.* High-accuracy classification of invasive weed seeds with highly similar morphologies: utilizing hierarchical bilinear pooling for fine-grained image classification. *Smart Agric Technol.* 2025;10:100758.

   https://doi.org/10.1016/j.atech.2024.100758

8. Luo Y, Xu S, Yuan H, Liu S, Xue H, Sun G. SeedStudio: a unified system for automated seed imaging and continual classification. *Comput Electron Agric.* 2026;247:111713.

   https://doi.org/10.1016/j.compag.2026.111713

9. Borgohain R, Goswami G, Das J, Khandai S, Tyagi NK, Chakrawarti N. Explaining grain quality trait importance and classification of traditional rice cultivars of Assam, India using SHAP-enhanced Random Forest, XGBoost, and Support Vector Machine models. *J Cereal Sci.* 2026;129:104457.

   https://doi.org/10.1016/j.jcs.2026.104457

10. Li L, Liu CZ, Cao K, Zhou Z, Alrowaily M. Artificial intelligence of things for smart agriculture with optimal embedded edge intelligence. *Comput Electr Eng.* 2026;133:111039.

    https://doi.org/10.1016/j.compeleceng.2026.111039

11. Pintus M, Colucci F, Maggio F. Emerging developments in real-time edge AIoT for agricultural image classification. *IoT.* 2025;6(1):13.

    https://doi.org/10.3390/iot6010013

12. Zhao H, Fu C, Zhang Y, Zhu W, Lu K, Francis EM. Dimensional decomposition-aided metamodels for uncertainty quantification and optimization in engineering: a review. *Comput Methods Appl Mech Eng.* 2024;428:117098.

    https://doi.org/10.1016/j.cma.2024.117098

13. Aristizábal-Alzate CE, Castillejos-López E, Dongil AB, Romero-Sáez M. Integration of design of experiments, analysis of variance and response surface methodology in assessing heterogeneous catalysts processes: a minireview. *ChemistryOpen.* 2024;14(1).

    https://doi.org/10.1002/open.202400148

14. Liu S, Wang H, Peng W, Yao W. Surrogate-assisted evolutionary algorithms for expensive combinatorial optimization: a survey. *Complex Intell Syst.* 2024;10(4):5933-5949.

    https://doi.org/10.1007/s40747-024-01465-5

15. Zhao G, Jiang W, Wu J, Chen B, Zhang L. Online evolutive learning for real-time image processing: a survey. *J Real-Time Image Proc.* 2026;23(5).

    https://doi.org/10.1007/s11554-026-01938-5

16. Chand HV, Onyema EM, Shieh CS, Jiang W, Kumar SA, Gupta SK. Multi-level ensemble learning using CNN feature aggregation for dermatological image classification. *Int J Comput Intell Syst.* Published online 2026.

    https://doi.org/10.1007/s44196-026-01427-4

17. Sulistya YI, Istighosah M, Septiara M, Septiadi AD, Amrullah A. Classification of noni fruit ripeness using Support Vector Machine (SVM) method. *IJODAS.* 2024;5(3):206-215.

    https://doi.org/10.56705/ijodas.v5i3.180

18. Qi H, Huang Z, Sun Z, *et al.* Rice seed vigor detection based on near-infrared hyperspectral imaging and deep transfer learning. *Front Plant Sci.* 2023;14.

    https://doi.org/10.3389/fpls.2023.1283921

19. Zhang Z. Multi-objective optimization method for building energy-efficient design based on multi-agent-assisted NSGA-II. *Energy Inform.* 2024;7(1).

    https://doi.org/10.1186/s42162-024-00394-4

20. Wang H, Liang Q, Hancock JT, Khoshgoftaar TM. Feature selection strategies: a comparative analysis of SHAP-value and importance-based methods. *J Big Data.* 2024;11(1).

    https://doi.org/10.1186/s40537-024-00905-w

21. Heidari A, Navimipour NJ, Unal M. Applications of ML/DL in the management of smart cities and societies based on new trends in information technologies: a systematic literature review. *Sustain Cities Soc.* 2022;85:104089.

https://doi.org/10.1016/j.scs.2022.104089

22. Amiri Z, Heidari A, Navimipour NJ, Unal M, Mousavi A. Adventures in data analysis: a systematic review of deep learning techniques for pattern recognition in cyber-physical-social systems. *Multimed Tools Appl.* 2023;83(8):22909-22973.

https://doi.org/10.1007/s11042-023-16382-x

23. Nabudda K, Poungthong P, Ritthong W, Elumalai PV. Physics-guided CFD–ML framework for sustainable classical wire coating with power-law fluids. *Eng.* 2026;7(7):352.

https://doi.org/10.3390/eng7070352

24. Phumpho S, Nabudda K, Poungthong P, Artnaseaw A. CFD-based thermodynamic stability and energy performance optimization of a refrigerated truck compartment using experimental validation and surrogate modelling. *Eng.* 2026;7(8):393.

https://doi.org/10.3390/eng7080393

25. Chakraborty SK, A S, Dubey K, *et al.* Development of an optimally designed real-time automatic citrus fruit grading–sorting machine leveraging computer vision-based adaptive deep learning model. *Eng Appl Artif Intell.* 2023;120:105826.

https://doi.org/10.1016/j.engappai.2023.105826

26. Zhou Z, Zahid U, Majeed Y, *et al.* Advancement in artificial intelligence for on-farm fruit sorting and transportation. *Front Plant Sci.* 2023;14.

https://doi.org/10.3389/fpls.2023.1082860

27. Hinterleitner A, Schulz R, Hans L, *et al.* Online machine learning and surrogate-model-based optimization for improved production processes using a cognitive architecture. *Appl Sci.* 2023;13(20):11506.

https://doi.org/10.3390/app132011506

28. He C, Zhang Y, Gong D, Ji X. A review of surrogate-assisted evolutionary algorithms for expensive optimization problems. *Expert Syst Appl.* 2023;217:119495.

https://doi.org/10.1016/j.eswa.2022.119495

29. Luo J, Ma X, Ji Y, Li X, Song Z, Lu W. Review of machine learning-based surrogate models of groundwater contaminant modeling. *Environ Res.* 2023;238(pt 2):117268.

https://doi.org/10.1016/j.envres.2023.117268

30. Majeed Y, Ojo MO, Zahid A. Standalone edge AI-based solution for tomato diseases detection. *Smart Agric Technol.* 2024;9:100547.

https://doi.org/10.1016/j.atech.2024.100547

31. Araújo GR, Gomes R, Gomes MG, Guedes MC, Ferrão P. Surrogate models for efficient multi-objective optimization of building performance. *Energies.* 2023;16(10):4030.

https://doi.org/10.3390/en16104030

32. Ritthong W, Elumalai PV, Promprasansuk S, Phasinam K, Albutt N, Poungthong P. Hybrid passive–active cooling using a single closed two-phase cooling system integrated with forced aeration for thermal stabilization and humidity control in paddy storage. *AgriEngineering.* 2026;8(9):399.

https://doi.org/10.3390/agriengineering8090399

33. Ritthong W, Chalernphon K, Kunla N, Poungthong P, Albutt N, Boonpunya A, Shabaz M, Phasinam K. Development and field validation of a solar-powered smart buoy for saltwater intrusion monitoring. *Solar.* 2026;6(5):67.

https://doi.org/10.3390/solar6050067

34. Mukhtar A, Yasir ASHM, Nasir MFM. A machine learning-based comparative analysis of surrogate models for design optimisation in computational fluid dynamics. *Heliyon.* 2023;9(8):e18674.

https://doi.org/10.1016/j.heliyon.2023.e18674

35. Huang Z, Wang R, Cao Y, *et al.* Deep learning based soybean seed classification. *Comput Electron Agric.* 2022;202:107393.

https://doi.org/10.1016/j.compag.2022.107393

36. Xu P, Tan Q, Zhang Y, Zha X, Yang S, Yang R. Research on maize seed classification and recognition based on machine vision and deep learning. *Agriculture.* 2022;12(2):232.

https://doi.org/10.3390/agriculture12020232

37. Alabbasy FM, Abohamama AS, Alrahmawy MF. Compressing medical deep neural network models for edge devices using knowledge distillation. *J King Saud Univ Comput Inf Sci.* 2023;35(7):101616.

https://doi.org/10.1016/j.jksuci.2023.101616

38. Žalik KR, Žalik M. A review of federated learning in agriculture. *Sensors (Basel).* 2023;23(23):9566.

https://doi.org/10.3390/s23239566

39. Khurana K, Sonsare P, Borkar D, Thakkar H, Bhagat O. MOLO: a hybrid approach using MobileNet and YOLO for object detection on resource constrained devices. *Discov Artif Intell.* 2025;5(1).

https://doi.org/10.1007/s44163-025-00398-3

40. Wijnker E, Bouchaut D, van Treuren R, van Hintum T. A pragmatic protocol for seed viability monitoring in ex situ plant genebanks. *Genet Resour Crop Evol.* 2024;72(1):49-59.

https://doi.org/10.1007/s10722-024-02019-x

Kriengkrai Nabudda *is a researcher specializing in Industrial Engineering at the School of Engineering, King Mongkut's Institute of Technology Ladkrabang (KMITL), Thailand. His primary research interests include 3D printing, mathematical modeling, numerical simulation, optimization, computational fluid dynamics, nonlinear viscoelasticity, and finite element analysis. His research further encompasses the application of mathematical and computational methods to solve complex engineering problems and analyze dynamical systems.*
https://orcid.org/0000-0003-2338-1443

Natakorn Thasnas *received his B.Eng. in Electrical Engineering from Khon Kaen University, Thailand, in 2003; his M.Eng. in Energy from the Asian Institute of Technology, Thailand, in 2007; and his Ph.D. in Electrical Engineering from Khon Kaen University, Thailand, in 2019. He is currently an Assistant Professor in the Department of Electrical and Computer Engineering, Faculty of Science and Engineering, Kasetsart University, Chalermphrakiat Sakon Nakhon Province Campus, Thailand. His research interests include advanced and intelligent control systems, optimization techniques, artificial intelligence and machine learning for control applications, and real-time industrial automation. His current research focuses on the development and application of intelligent control and optimization techniques for smart agricultural systems, with an emphasis on improving automation, operational efficiency, and system performance.*
https://orcid.org/0000-0002-4957-5126

Elumalai Perumal Venkatesan *is currently a Professor at Aditya University, Andhra Pradesh, India. He earned his B.E. in Mechanical Engineering from Anna University, Chennai, India, in 2011; his M.E. in Manufacturing Engineering from Anna University in 2013; and his Ph.D. in Automobile Engineering from Anna University in 2020. He also completed a postdoctoral fellowship at the National Kaohsiung University of Science and Technology, Taiwan, in 2025. His research interests include internal combustion engines, alternative fuels, biofuels, sustainable energy technologies, computational fluid dynamics, thermal engineering, numerical simulation, and engineering optimization. His research further encompasses the application of artificial intelligence, machine learning, and response surface methodology for predictive modeling, performance optimization, and the development of energy-efficient engineering systems. He has extensive experience in experimental and computational research, with particular emphasis on sustainable technologies, intelligent engineering applications, and data-driven optimization.*
https://orcid.org/0000-0002-7536-8200

Sutham Craivanich *is a retired government official and engineering consultant associated with Srithaidoem Group Co., Ltd., Thailand. He earned his B.Eng. in Civil Engineering from Khon Kaen University, Thailand, in 1968, and his M.Sc. in Civil Engineering from the University of Texas at Arlington, USA, in 1973. He has extensive professional experience in civil engineering and engineering consultancy. Since 2020, he has served as a consultant, applying his engineering knowledge and professional experience to various technical and industrial activities. His areas of expertise include civil engineering and engineering consultancy, with a particular interest in the practical application of engineering principles to industrial and technological development.*

Pongthep Poungthong *is a Lecturer in Industrial Engineering at the School of Engineering, King Mongkut's Institute of Technology Ladkrabang (KMITL), Thailand. His primary research interests include fractional calculus, mathematical modeling, numerical simulation, optimization, computational fluid dynamics, nonlinear viscoelasticity, non-Newtonian fluid mechanics, rheology, and transport phenomena. His research further focuses on the application of mathematical and computational methods to complex engineering problems and dynamical systems, particularly surrogate modeling, computational optimization, data-driven prediction, and the development of efficient numerical frameworks for engineering and industrial applications.*
https://orcid.org/0000-0002-5278-5984

Suwilai Phumpho *is a Lecturer in the Department of IoT and Information Engineering at King Mongkut's Institute of Technology Ladkrabang (KMITL), Thailand, and a member of the Thai parliamentary Subcommittee on Science, Research, and Innovation. He received his Ph.D. degree in Electrical Engineering from KMITL under the prestigious Royal Golden Jubilee (RGJ) Ph.D. Scholarship program. He previously earned his M.Eng. in Information Engineering from the same institute and his B.Eng. in Electronic Engineering with first-class honors from Mahanakorn University of Technology (MUT). As a licensed Professional Engineer with expertise in advanced engineering technologies, he provides consultancy services to leading technology and energy firms. His research interests include Artificial Intelligence of Things (AIoT), digital twin applications, operational technology (OT) security, industrial automation, and energy solutions.*
https://orcid.org/0009-0001-9590-8307



This work is licensed under a Creative Commons Attribution 4.0 International License. The authors retain ownership of the copyright for their article, but they allow anyone to download, reuse, reprint, modify, distribute, and/or copy articles in IJOCTA, so long as the original authors and source are credited. To see the complete license contents, please visit http://creativecommons.org/licenses/by/4.0/.